European Journal of Medicinal Chemistry 219 (2021) 113429

Contents lists available at ScienceDirect

European Journal of Medicinal Chemistry

journal homepage: http://www.elsevier.com/locate/ejmech

Research paper

Synthesis and structure–activity relationship study of novel 3-diethoxyphosphorylfuroquinoline-4,9-diones with potent antitumor efficacy

Jakub Modranka [a, 1], Joanna Drogosz-Stachowicz [b, 1], Anna Pietrzak [c], Anna Janecka [b, **], Tomasz Janecki [a, *]

[a] Institute of Organic Chemistry, Lodz University of Technology, Żeromskiego 116, 90-924, Łódź, Poland
[b] Department of Biomolecular Chemistry, Medical University of Łódź, Mazowiecka 6/8, 92-215, Łódź, Poland
[c] Institute of General and Ecological Chemistry, Lodz University of Technology, Żeromskiego 116, 90-924, Łódź, Poland

ARTICLE INFO

Article history:
Received 19 February 2021
Received in revised form
27 March 2021
Accepted 27 March 2021
Available online 3 April 2021

Keywords:
Quinolinediones
Phosphonates
Hybrid molecules
Cytotoxic activity
Apoptosis
DNA damage

ABSTRACT

Herein we report an efficient synthesis of a series of regioisomeric *N,O-syn* and *N,O-anti* 3-diethoxyphosphorylfuroquinoline-4,9-diones combining furoquinoline-5,8-dione skeleton, present in several highly cytotoxic compounds, with diethoxyphosphoryl moiety. The cytotoxic activity of the obtained analogs was tested against two human cancer cell lines: promyelocytic leukemia HL-60 and breast cancer adenocarcinoma MCF-7 and for comparison on human umbilical vein endothelial cells HUVEC and mammary gland/breast MCF-10 A cells. Several diethoxyphosphorylfuroquinoline-4,9-diones proved to be highly cytotoxic for cancer cells with IC_{50} values even below 0.1 μM. Interestingly, *N,O-syn* 3-diethoxyphosphorylfuroquinoline-4,9-diones were 3- to 7-fold more active against HL-60 cells than the respective *N,O-anti* regioisomers. The most promising analogs **9c** and **9i**, with the highest cancer/healthy cells cytotoxicity ratio, were further evaluated to establish their mode of action. In HL-60 cells these analogs enhanced intracellular ROS generation and NAD(P)H:quinone oxidoreductase 1 (NQO1) depletion which led to the cell cycle arrest in the S-phase, reduced cell proliferation, DNA damage and apoptosis.
© 2021 The Author(s). Published by Elsevier Masson SAS. This is an open access article under the CC BY license (http://creativecommons.org/licenses/by/4.0/).

1. Introduction

It is well established that nitrogen-containing heterocycles are found in various natural products, biologically active structures, and medicinally relevant compounds [1–3]. Among them, quinoline-5,8-diones have gained considerable attention in medicinal chemistry, due to the fact that compounds containing such skeleton possess multiple biological properties, including antimicrobial, antiprotozoan and anticancer activity [4–6]. This structural motif can be found in antitumor antibiotics, such as streptonigrin **1** and its derivatives [7] (Fig. 1). Natural ascidiathiazone A **2,** obtained from a New Zealand ascidian *Aplidium* species, is a growth inhibitor of some parasitic protozoa, e.g. *Trypanosoma brucei rhodesiense* [8] and benzofuroquinoline-5,8-diones **3** were identified as topoisomerase II inhibitors and their cytotoxicity against several types of human cancer cell lines was similar or higher than that of doxorubicin [9]. Also, furoquinoline-5,8-diones **4** were reported as compounds having high cytotoxic activity against cancer cells, as well as cancer stem cells [10]. It is worth to stress that the authors didn't notice major differences in the activity between *N,O-anti* and *N,O-syn* isomers. Recently, furoquinoline-5,8-diones **5** have been identified as effective tyrosyl-DNA phosphodiesterase 2 (TDP2) inhibitors [11] and many analogs of **5** were designed to probe various substituents at position 3 and alternations in the furan ring motif.

On the other hand, phosphorus-substituted heterocycles have received considerable attention mainly due to their synthetic applications and growing usefulness in drug design [12–14]. There are numerous reports claiming that the presence of phosphoryl group can enhance biological activity. It can mimic the tetrahedral intermediates formed in enzymatic reactions involved in the

* Corresponding author.
** Corresponding author.
E-mail addresses: anna.janecka@umed.lodz.pl (A. Janecka), tomasz.janecki@p.lodz.pl (T. Janecki).
[1] J.M and J. D-S. contributed equally.

https://doi.org/10.1016/j.ejmech.2021.113429
0223-5234/© 2021 The Author(s). Published by Elsevier Masson SAS. This is an open access article under the CC BY license (http://creativecommons.org/licenses/by/4.0/).

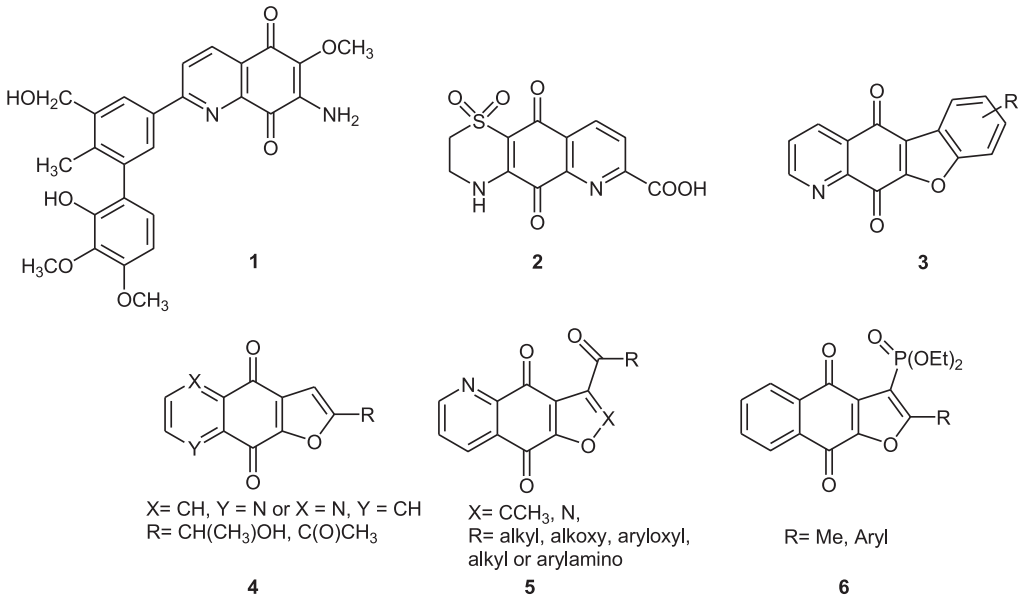

Fig. 1. Structures of some natural and synthetic quinoline-5,8-diones.

carboxyl group metabolism [13,15,16] and this rationale has resulted in the design of some important drugs [17], such as N-phosphonoacetyl-L-aspartic acid (PALA) with anticancer activity or fosinopril which is a clinically useful antihypertensive agent. Furthermore, it was shown that the presence of dialkoxy or diaryloxyphosphoryl group may improve bioavailability of drugs [18] and also influence cancer progression through the inhibition of farnesyl protein transferase [19,20] or purine nucleoside phosphorylase [21,22].

From some time in our laboratory we have been developing methods for the synthesis of phosphorylated oxa- and azaheterocycles, as a valuable group of synthetically and biologically important compounds [23,24]. Recently, we have designed a series of 3-diethoxyphosphorylnaphthofuran-4,9-diones **6**, which integrated the merits of both, a phosphoryl group and naphthofuran-4,9-dione skeleton. These compounds showed high cytotoxic activity against leukemia HL-60, NALM-6 and breast cancer MCF-7 cell lines, with IC_{50} values below 10 μM [25]. Now, we decided to examine, whether the incorporation of the nitrogen atom into the naphthofuran-4,9-dione moiety might enhance the cytotoxic activity of these compounds. Therefore, in this paper we report the synthesis and anticancer evaluation of a series of *N,O-syn* and *N,O-anti* 3-diethoxyphosphorylfuroquinoline-4,9-diones **9** and **10**, respectively, containing a variety of substituents in position 2.

2. Results and discussion

2.1. Chemistry

The 3-diethoxyphosphorylfuroquinoline-4,9-diones **9a-i** and **10a-i** were obtained from 6,7-dichloroquinoline-5,8-dione (**7**) and β-ketophosphonates **8**, applying the procedure previously described for the synthesis of 3-diethoxyphosphorylnaphthofuran-4,9-diones **6** [25] (Scheme 1). 6,7-Dichloroquinoline-5,8-dione (**7**) was synthesized by oxidizing 8-hydroxyquinoline with sodium chlorate in the concentrated HCl solution [26], phosphonates **8a-b** were commercially available and phosphonates **8c-i** were prepared using literature procedure [25]. All reactions proceeded smoothly and yielded mixtures of *N,O-syn* and *N,O-anti* regioisomers **9** and **10**, respectively. These mixtures were successfully separated by column chromatography to give pure **9** and **10** in yields given in Table 1. Structures of all obtained compounds were confirmed by ^{1}H, ^{13}C and ^{31}P NMR spectra. Distinction between *N,O-syn* and *N,O-anti* regioisomers **9i** and **10i** was made using X-ray analysis.

Yellow crystals of two isomers of **9i** and **10i** were obtained by slow evaporation of ethyl acetate. Their crystal structures were determined by low temperature (100 K) single crystal X-ray analysis. Molecular conformations of **9i** and **10i** are shown in Fig. 2.

Regiochemistry of the remaining 3-diethoxyphosphorylfuro quinoline-4,9-diones **9a-h** and **10a-h** was assigned on the basis of the similarities of their ^{13}C and ^{31}P NMR spectra to the spectra of **9i** and **10i**, respectively. For example, in ^{13}C NMR spectrum of **9i**, C-4a atom (Fig. 2) has chemical shift of 130.48 and chemical shifts of this atom in all *syn*-regioisomers **9a-h** are very similar and fall within the range from 130.37 to 130.64. Accordingly, chemical shifts of C-8a atoms in **10a-h** fall within the range from 128.74 to 128.85 and the chemical shift of this atom in **10i** is 128.85. In ^{31}P NMR spectra *syn*-regioisomer **9i** has greater chemical shift value than *anti*-regioisomer **10i** (6.16 and 5.84, respectively) therefore *syn*-regiochemistry can be assigned to all these regioisomers in pairs, which had greater chemical shift value in ^{31}P NMR spectrum.

2.2. Biology

2.2.1. Cytotoxic activity of novel hybrids against cancer and normal cell lines

The synthesized *N,O-syn* and *N,O-anti* 3-diethoxyphosph orylfuroquinoline-4,9-diones **9** and **10** were tested *in vitro* against two human cancer cell lines: promyelocytic leukemia HL-60 and breast cancer adenocarcinoma MCF-7 and the most cytotoxic analogs also against human umbilical vein endothelial cells HUVEC and mammary gland/breast MCF-10 A cells for 48 h. The obtained results, which are shown in Table 2, were compared with doxorubicin used as a positive control. All tested compounds were highly cytotoxic for HL-60 cells, with IC_{50} values below 1 μM, and in case of analogs **9c,f,h** even below 0.1 μM (IC_{50} for doxorubicin = 0.11 μM). The IC_{50} values obtained in MCF-7 cells were also very low and varied from below 0.1 μM for **9c,g,h** to 1.59 μM for **9b** (IC_{50} for doxorubicin = 0.89 μM). All

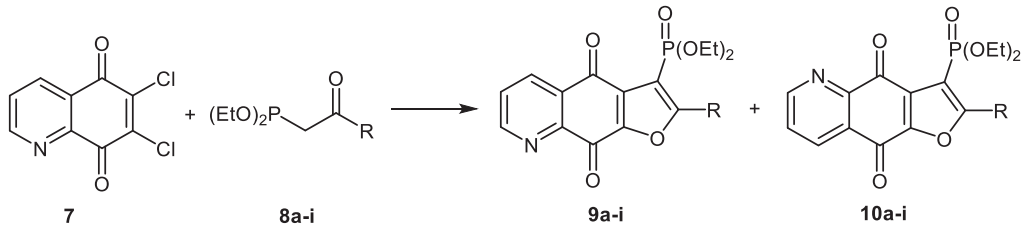

Scheme 1. Synthesis of 3-diethoxyphosphorylfuroquinolinedione isomers **9a-i** and **10a-i.**

Table 1
Yields of *N,O-syn* and *N,O-anti* 3-dietoxyphosphorylfuroquinoline-4,9-diones **9** and **10**.

9 or 10	R	Yield [%][a]	
		9	10
a	Me	12	18
b	Ph	32	28
c	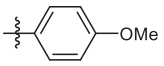	21	22
d	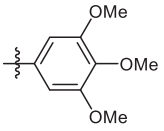	25	25
e	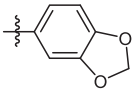	23	26
f	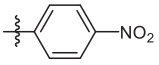	19	28
g	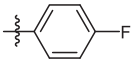	26	26
h	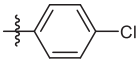	26	26
i	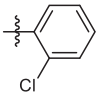	22	27

[a] Yields of pure, separated products based on **7**.

the most active compounds with IC_{50} below 0.1 μM had phenyl substituent containing either electron withdrawing groups (*p*-NO_2, **9f**; *p*-F, **9g**; *p*-Cl, **9h**) or electron donating group (*p*-OMe, **9c**). Apparently, there is no simple correlation between electron density of the phenyl ring and cytotoxic activity. On the other hand, *syn* or *anti* relationship between furan oxygen and quinoline nitrogen atoms is important for the activity. *N,O-syn* 3-diethoxyphosphorylfuroquinoline-4,9-diones **9b-h** were 3- to 7-fold more active in HL-60 cells than the respective *N,O-anti* regioisomers **10b-h**. Only **9a,i** were equipotent with **10a,i**. This relationship can be also observed in MCF-7 cell line. The most active *N,O-syn* diethoxyphosphorylfuroquinoline-4,9-diones **9c,g,h** were 4- to 12-fold more active against MCF-7 cells than their *N,O-anti* regioisomers **10c,g,h**. Although the reason for the enhanced activity of *N,O-syn* regioisomers is not clear it might be speculated that they may better fit into the binding site of the protein.

Selected 3-diethoxyphosphorylfuroquinoline-4,9-diones were also tested on HUVEC and MCF-10 A, to evaluate their influence on normal cells. The most pronounced difference in cytotoxicity between cancer and normal cells was observed for 2-(4-methoxyphenyl)-3-diethoxyphosphorylfuroquinoline-4,9-dione **9c** which was 12-fold less toxic for HUVEC than HL-60 cells. The same compound was also 5-fold less toxic for normal MCF-10 A than cancer MCF-7 cells.

The presented data clearly showed that the incorporation of a nitrogen atom into the naphthofuran-4,9-dione moiety enhanced the cytotoxicity. Comparison of the cytotoxic activity of formerly published 3-diethoxyphosphorylnaphthofuran-4,9-diones **6a-c** (**6a**, R = Me; **6b**, R = Ph; **6c**, R = 2-chlorophenyl) [25] (Table 2) with 3-diethoxyphosphorylfuroquinoline-4,9-diones **9** or **10** showed that the latter ones were 15- to 30-fold more active in HL-60 cells and 2- to 5-fold more active in MCF-7 cells. For example, 2-phenyl-3-diethoxyphosporylfuroquinoline-4,6-dione **9b** (IC_{50} = 0.20 μM) was 30-fold more active than 2-phenyl-3-diethoxyphospory lnaphthalene-4,9-dione **6b** (IC_{50} = 6.01 μM) in HL-60 cells. Also

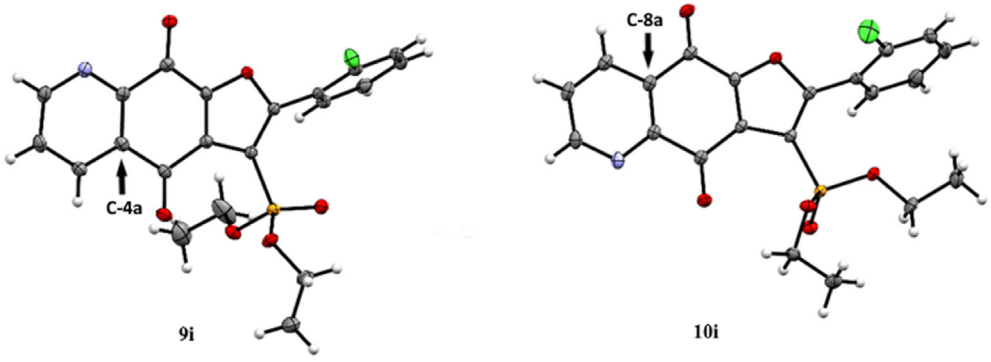

Fig. 2. Molecular structures of isomers **9i** and **10i.**

Table 2
In vitro cytotoxic activity of 3-diethoxyphosphorylfuroquinoline-4,9-diones **9a-i**, **10a-i** and 3-diethoxyphosphorylnaphthofuran-4,9-diones **6a-c** tested on two cancer and two normal cell lines.

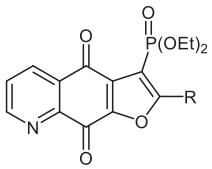

9a-i

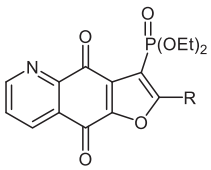

10a-i

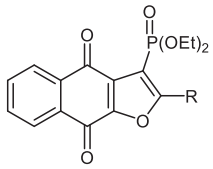

6a, R = Me
6b, R = Ph
6c, R = 2-ClC$_6$H$_4$

No	IC_{50}[a] (μM)					
	HL-60	MCF-7	HUVEC	MCF-10 A	HUVEC/HL-60	MCF-10 A/MCF-7
9a	0.84 ± 0.01	1.59 ± 0.05	2.88 ± 0.12	8.28 ± 0.19	3.4	5.2
10a	0.94 ± 0.01	5.94 ± 0.01	3.07 ± 0.11	11.10 ± 0.57	3.3	1.9
9b	0.20 ± 0.01	1.59 ± 0.01	1.68 ± 0.01		8.4	
10b	0.76 ± 0.01	1.10 ± 0.01	0.38 ± 0.01		0.5	
9c	0.09 ± 0.00	0.10 ± 0.01	1.05 ± 0.045	0.50 ± 0.01	12	5
10c	0.63 ± 0.01	1.21 ± 0.04	0.34 ± 0.01		0.5	
9d	0.30 ± 0.02	1.50 ± 0.16	0.42 ± 0.01		1.4	
10d	0.72 ± 0.01	0.98 ± 0.02	1.82 ± 0.08	5.37 ± 0.11	2.5	5.5
9e	0.16 ± 0.01	0.95 ± 0.03	0.10 ± 0.01		0.6	
10e	0.65 ± 0.01	1.15 ± 0.04	0.39 ± 0.01		0.6	
9f	0.07 ± 0.01	1.32 ± 0.01	0.09 ± 0.01		1.3	
10f	0.41 ± 0.02	0.76 ± 0.01	0.33 ± 0.01		0.8	
9g	0.13 ± 0.01	0.08 ± 0.01	0.55 ± 0.02	0.33 ± 0.01	4.2	4
10g	0.39 ± 0.01	0.74 ± 0.01	1.00 ± 0.001	3.42 ± 0.01	2.6	4.6
9h	0.09 ± 0.01	0.09 ± 0.01	0.11 ± 0.01	0.27 ± 0.03	1.1	3
10h	0.37 ± 0.01	0.35 ± 0.01	0.27 ± 0.01		0.7	
9i	0.37 ± 0.01	0.48 ± 0.01	1.11 ± 0.03	3.29 ± 0.09	3	6.9
10i	0.38 ± 0.01	0.54 ± 0.02	0.33 ± 0.01	2.45 ± 0.12	0.86	4.5
6a[b]	8.13 ± 0.16	5.70 ± 0.21				
6b[b]	6.01 ± 0.18	2.40 ± 0.30				
6c[b]	6.35 ± 0.46	2.34 ± 0.18	3.73 ± 0.18	10.03 ± 0.43	2	4
Dox	0.11 ± 0.01	0.89 ± 0.12	3.8 ± 0.45	1.37 ± 0.28	34	1.5

[a] Compound concentration required to inhibit cell proliferation by 50% after 48 h treatment. Data are expressed as the mean ± SEM from the concentration-response curves of at least three experiments.
[b] Data taken from the reference [25].

cancer/healthy cells IC_{50} ratio was in favor of 3-diethoxyphosporylfuroquinoline-4,6-diones. When 2-(2-chlorophenyl)-3-diethoxyphosporylfuroquinoline-4,6-dione **9i** was compared with 2-(2-chlorophenyl)-3-diethoxyphosporylnaphthalene-4,9-dione **6c** the first one was 3-fold less toxic in HUVEC than HL-60 cells and 7-fold less toxic in MCF-7A than MCF-7 cells. Corresponding values for 2-(2-chlorophenyl)-3-diethoxyphosporylnaphthalene-4,9-dione **6c** were 2 and 4, respectively.

The most promising analogs **9c** and **9i**, with the highest cancer/healthy cells cytotoxicity ratio, were chosen for further evaluation in order to establish their mode of action. Cytotoxicity of these two compounds in HL-60 cells was then assessed after 24 h incubation. Both compounds showed high cytotoxic activity with IC_{50} = 0.11 μM for **9c** and IC_{50} = 0.11 μM for **9i** (Fig. 3 A).

2.2.2. Cell cycle arrest

The cell cycle arrest is a mechanism by which anticancer drugs may exert their cytotoxic action. The cell cycle distribution was assessed by DNA staining with DAPI followed by flow cytometry analysis. HL-60 cells were exposed to **9c** (at IC_{50}, $2IC_{50}$ and $4IC_{50}$ concentrations) and **9i** (at IC_{50} and $2IC_{50}$ concentrations). Both compounds significantly induced the cell cycle arrest in S phase (47.9 ± 0.71%, 50.8 ± 0.5%, 60.0 ± 0.9% and 40.6 ± 0.6%, 47.5 ± 2.27%, respectively), while population of cells in G0/G1 and G2/M phases was diminished. Moreover, treatment with **9c** (at $2IC_{50}$ and $4IC_{50}$ concentrations) and **9i** (at IC_{50} and $2IC_{50}$concentrations) caused also a significant subG0/G1 cell cycle arrest in 6.6 ± 0.4%, 14.3 ± 0.9% and 6.7 ± 0.8%, 16.9 ± 0.4% cells, respectively (Fig. 3 D, E).

2.2.3. Antiproliferative activity

The S-phase of the cell cycle is a part of the interphase in which replication of DNA takes place [27]. However, considering that the tested compounds decreased the cells' metabolic activity, the increase of number of cells in the S phase was most likely not caused by the increase in cell population actively replicating DNA, but rather due to accumulation of cells with arrested progress in this phase. To confirm this hypothesis, the ability of **9c** and **9i** to inhibit HL-60 cell proliferation was evaluated by exposure of cells to 5-bromodeoxyuridine (BrdU), a thymidine analog that incorporates into newly synthesized DNA during the S-phase of the cell cycle, followed by flow cytometry analysis. The results showed that both compounds significantly decreased the population of actively cycling cells that incorporated BrdU. As presented in Fig. 3 B, C, treatment with **9i** at IC_{50} and $2IC_{50}$ concentrations for 24 h decreased proliferating cell population to 29.6 ± 2.4% and 1.4 ± 0.3%, respectively, whereas **9c** at IC_{50}, $2IC_{50}$ and $4IC_{50}$ concentrations caused reduction to 49.4 ± 2.7%, 20.4 ± 0.6% and 1.9 ± 0.2%, respectively, in comparison to control (86.0 ± 0.01%). The results indicated, that accumulation of cells in the S-phase caused by **9c** and **9i** treatment was simultaneous with decreased DNA synthesis and cell proliferation, hence cells' progression was arrested in the S-phase.

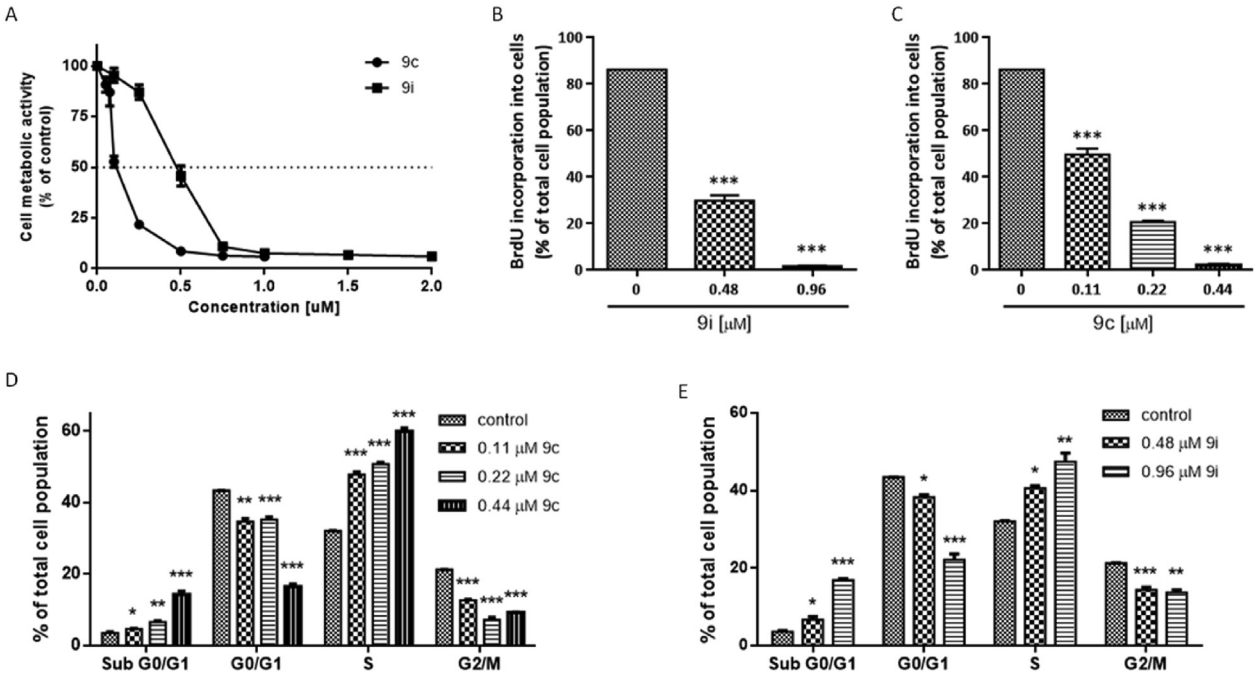

Fig. 3. Effect of **9c** and **9i** treatment on metabolic activity (A) cell proliferation (B, C) and cell cycle distribution (D, E) in HL-60 cells. A: Metabolic activity of HL-60 cells treated with **9c** and **9i** for 24 h assessed by MTT assay. The error bars represent mean of two independent experiments each preformed in triplicate ± SEM. B–E: Cells were exposed to **9c** (at IC_{50}, $2IC_{50}$ and $4IC_{50}$ concentrations) or to **9i** (at IC_{50} and $2IC_{50}$ concentrations) for 24 h, stained with BrdU and DAPI and analyzed by flow cytometry. The error bars represent mean of three replicates ±SEM. *p < 0.05, **p < 0.01, and ***p < 0.001 were considered significant in comparison to control.

2.2.4. Induction of apoptosis and DNA damage

The appearance of cells in sub-G0/G1 phase in the cell cycle analysis suggested induction of apoptosis in HL-60 cells by treatment with **9c** and **9i**. Hence, occurrence of 89 kDa fragment of cleaved-PARP, generated by cleavage of PARP1 by caspase 3 and 7 during caspase-mediated apoptosis [28], was investigated using Anti-Cleaved PARP (Asp214) antibodies and flow cytometry analysis (Fig. 4 D, E). **9c** at IC_{50}, $2IC_{50}$ and $4IC_{50}$ concentrations, dose-dependently increased the population of cells with cleaved PARP to 24.7 ± 3.2%, 46.6 ± 1.2% and 77.5 ± 1.8%, respectively. Treatment with **9i** at IC_{50} and $2IC_{50}$ concentrations also led to the significant PARP cleavage in 33.8 ± 2.1% and 81.0 ± 1.0% of cell population, respectively, compared to control (2.1 ± 0.4%). Moreover, pro-apoptotic activity of **9c** and **9i** was confirmed by Annexin V and Propidium iodide staining (Fig. 4A–C). In the control group, 91.1 ± 0.1% of HL-60 cells were healthy, 2.5 ± 0.1% were in early stage apoptosis (Annexin V-positive and PI-negative) and 6.1 ± 0.1% were in late stage apoptosis (both Annexin V and PI-positive). **9c** induced a small increase in the early apoptotic cells amount but the number of late apoptotic cells after exposure to IC_{50}, $1.5IC_{50}$ and $2IC_{50}$ concentrations of **9c** was more prominent (16.3 ± 0.9%, 22.5 ± 0.8%, 27.4 ± 2.0%, respectively). **9i** at IC_{50}, $1.5IC_{50}$ and $2IC_{50}$ concentrations significantly induced both, early stage apoptosis in 18.3 ± 0.6%, 21.2 ± 0.4% and 17.2 ± 1.0% cells, respectively, and late stage apoptosis in 37.4 ± 3.8%, 63.6 ± 0.2% and 68.4 ± 1.1% cells, respectively. The results indicate, that **9c** and **9i** significantly induced caspase-dependent apoptosis in HL-60 cells.

An early cells' response to DNA damage include the histone variant H2AX phosphorylation on Ser139, producing γH2AX, which is often used as a biomarker for DNA double-strand breaks (DSBs) detection [29,30]. Therefore, induction of DSBs was assessed by staining the HL-60 cells with γH2AX fluorescent antibody and flow cytometry analysis (Fig. 4 F, G). Exposure of cells to **9i** at IC_{50} and $2IC_{50}$ concentrations induced significant γH2AX generation in 13.8 ± 0.7% and 35.2 ± 0.6% of cells, respectively. **9c** was noticeably less genotoxic, leading to H2AX phosphorylation only in 3.6 ± 0.1% and 8.4 ± 0.1% cell population after treatment with **9c** at $2IC_{50}$ and $4IC_{50}$ concentrations, respectively, compared to control (2.2 ± 0.1%).

2.2.5. Induction of mitochondrial dysfunction

Mitochondrial transmembrane potential (ΔΨm) is considered a vital indicator of mitochondrial function and is usually used to assess the health of cells. Loss of ΔΨm is often observed in unhealthy or apoptotic cells. Detection of ΔΨm may be performed using JC-1 dye, which has an ability to enter the healthy cells' mitochondria, accumulate and form aggregates exhibiting red fluorescence. JC-1 dye does not form aggregates in unhealthy cells with low ΔΨm, which consequently show lower fluorescence [31]. To examine the influence of **9c** and **9i** treatment on ΔΨm status, HL-60 cells were stained with JC-1 fluorochrome and analyzed using flow cytometry. In the healthy, untreated HL-60 cells only 4.7 ± 0.5% of cells showed low red fluorescence. Treatment with **9c** at IC_{50}, $2IC_{50}$ and $4IC_{50}$ concentrations significantly increased the number of cells showing low ΔΨm to 43.4 ± 1.0%, 62.8 ± 0.7% and 85.7 ± 0.4% cell population, respectively. Similarly, **9i** (at IC_{50}, $2IC_{50}$ concentration) also induced mitochondrial depolarization in 47.2 ± 1.8% and 74.9 ± 0.6% of cells, respectively (Fig. 5 A, B).

2.2.6. Reactive oxygen species generation

Unlike normal cells, cancer cells exhibit increased ROS production due to elevated metabolic rate. However, cancer cells also demonstrate over-activated antioxidant systems that enable cell adaptation and ROS amount maintenance below toxic levels [32]. Excessive ROS generation or reduced antioxidant activity may cause oxidative stress leading to DNA, protein and lipid damage and eventually to cell death [33]. Many chemotherapeutic agents have been reported to cause apoptosis of cancer cells by substantial ROS increase. Thus, augmenting ROS production by exogenous compounds or inhibitors of ROS scavengers may be used as a therapeutic target in anticancer

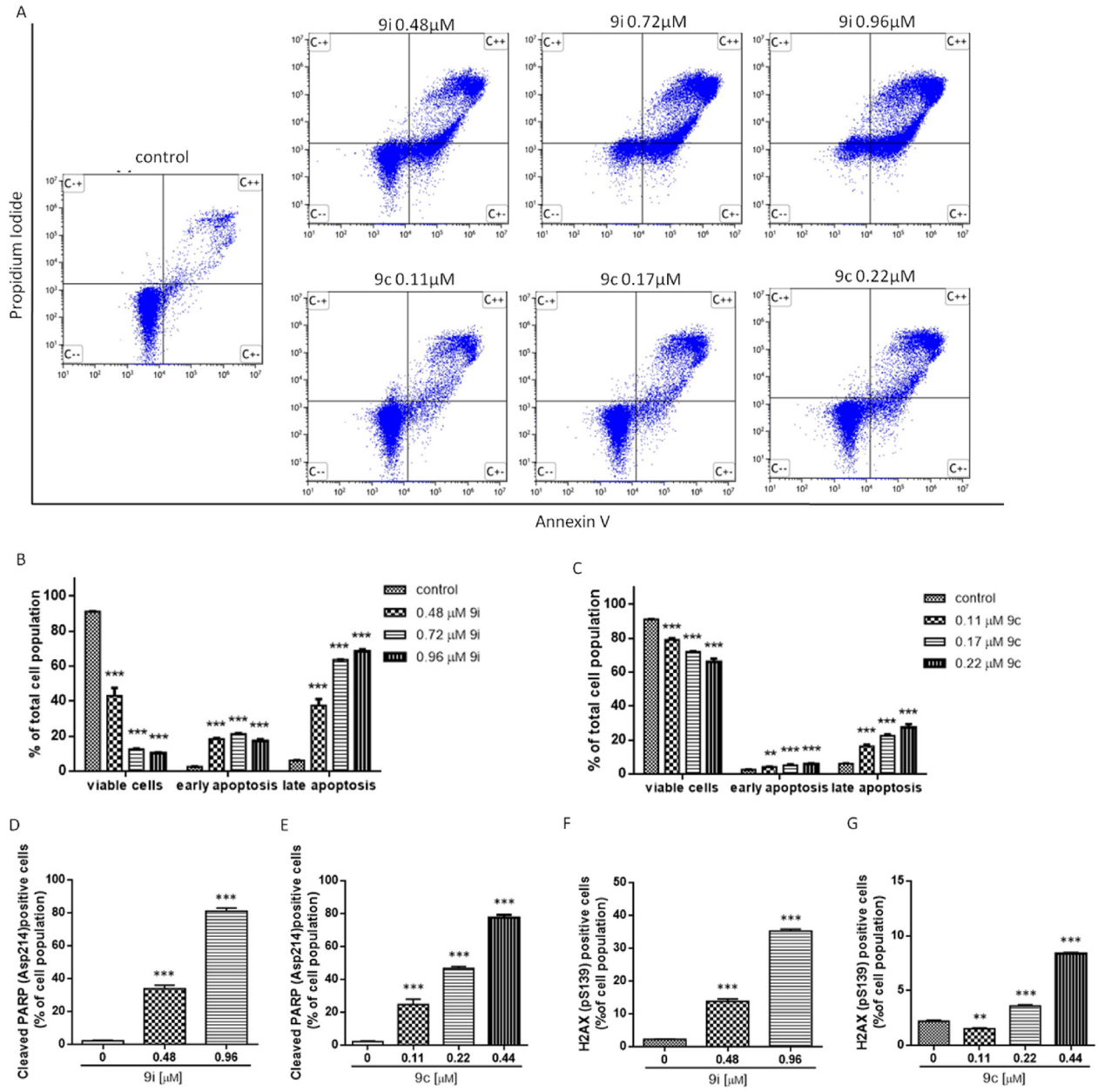

Fig. 4. Induction of apoptosis and DNA damage. A, B, C: HL-60 cells were exposed to **9c** and **9i** at IC_{50}, $1.5IC_{50}$ and $2IC_{50}$ concentrations for 24 h, stained with Annexin V and PI and analyzed by flow cytometry. D–G: Cells were treated with **9c** (IC_{50}, $2IC_{50}$ and $4IC_{50}$ concentrations) and **9i** (IC_{50} and $2IC_{50}$ concentrations) for 24 h, stained with PE Anti-Cleaved PARP (Asp214) and Anti-H2AX (pS139) antibodies and analyzed by flow cytometry. The error bars represent mean of three replicates ±SEM. *$p < 0.05$, **$p < 0.01$, and ***$p < 0.001$ were considered significant in comparison to untreated control.

drug development [34]. The influence of **9c** and **9i** on ROS generation in HL-60 cells was assessed by flow cytometry using CellROX Oxidative Stress Green Reagent (LifeTechnologies, Carlsbad, CA, USA) (Fig. 5C). Treatment with **9c** and **9i** at IC_{50} concentrations for 24 h significantly increased intracellular ROS production in 37.0 ± 4.7% and 72.5 ± 0.9% of cells, respectively. The results suggest that the investigated compounds induce oxidative stress in HL-60 cells which may cause the observed cytotoxic activity.

2.2.7. NQO1 activity alteration

The results of several studies indicate, that inhibition of antioxidant enzymes leads to apoptosis of cancer cells [35]. One of the cellular antioxidant systems, which is often overexpressed in several cancer tissues, is NAD(P)H:quinone oxidoreductase 1 (NQO1) [36]. Therefore, NQO1 may pose as a target for anticancer treatment development [37]. Additionally, recent studies imply that some quinolinediones are substrates of NQO1 and show selective cytotoxicity in cancer cell lines with upregulated NQO1 [38]. In our study, inhibitory activity against NQO1 was investigated using NQO1 activity assay kit (Abcam, Cambridge, MA, USA). Treatment with **9c** and **9i** at 0.1 μM, 0.5 μM and 1 μM for 24 h induced significant dose-dependent inhibition of NQO1 activity. **9c** was a more potent NQO1 inhibitor than **9i** (Fig. 5D). Therefore NQO1 depletion may sensitize cancer cells to oxidative stress, finally leading to reduced cell proliferation and apoptosis.

3. Conclusions

In this report, we described an efficient synthesis of a series of regioisomeric *N,O-syn* and *N,O-anti* 3-diethoxyphosphorylfuroq

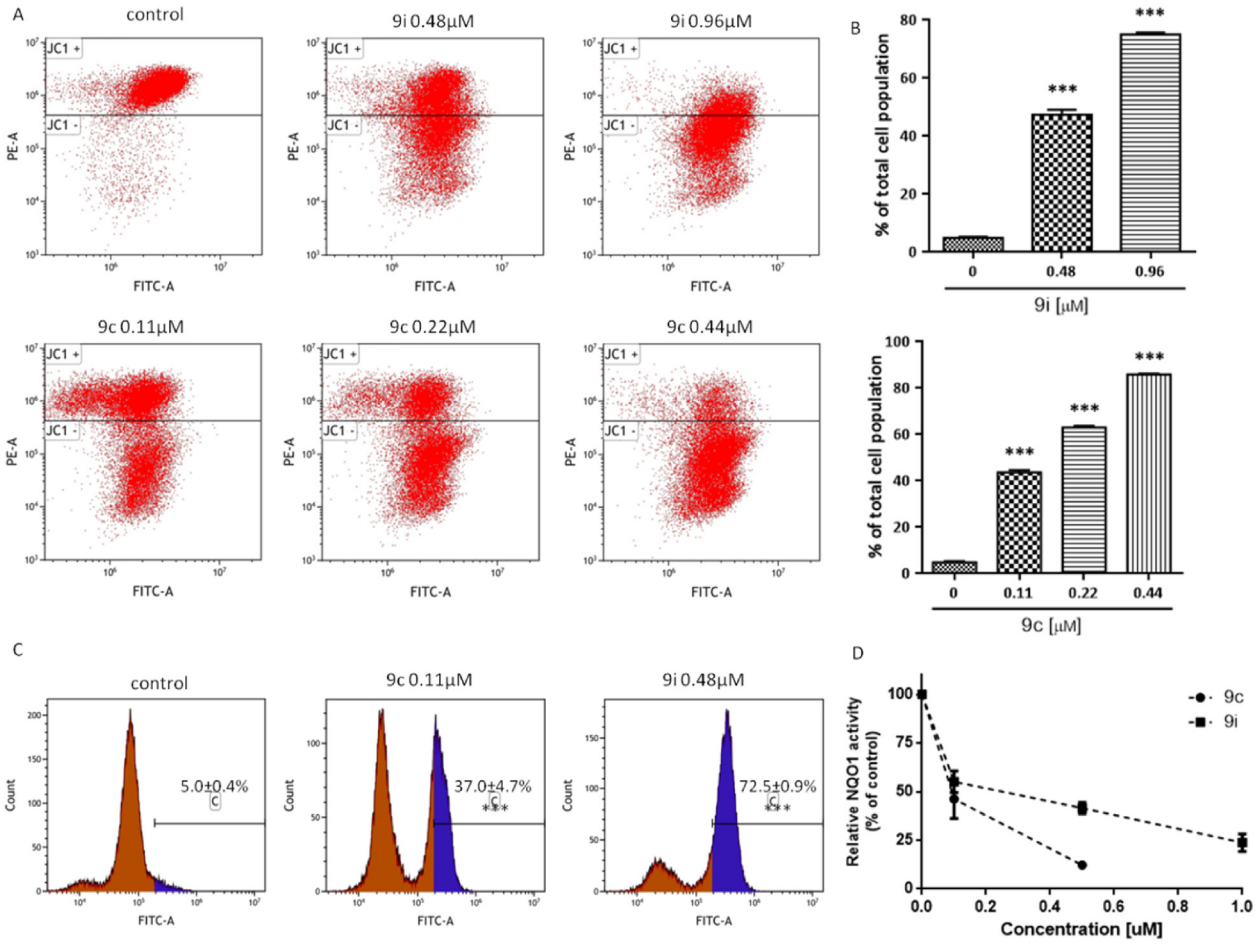

Fig. 5. A, B: Effect of **9c** and **9i** 24 h treatment on mitochondrial membrane potential in HL-60 cells. Cells were treated with **9c** (at IC_{50}, $2IC_{50}$ and $4IC_{50}$ concentrations) or **9i** (at IC_{50} and $2IC_{50}$ concentrations), stained with JC-1 dye and analyzed by flow cytometry. C: Effect of **9c** and **9i** on ROS formation in HL-60 cells. Cells were treated with IC_{50} concentrations of **9c** and **9i** for 24 h, stained with CellROX Green Reagent and analyzed by flow cytometry. D: NQO1 activity in HL-60 cells after compound treatment. Cells were treated with **9c** or **9i** (0.1 μM, 0.5 μM and 1 μM) for 24 h. NQO1 activity was assessed by the NQO1 activity assay kit (Abcam). The error bars represent mean of three replicates ±SEM. *$p < 0.05$, **$p < 0.01$, and ***$p < 0.001$ were considered significant in comparison to control.

uinoline-4,9-diones, combining furoquinoline-5,8-dione skeleton with diethoxyphosphoryl moiety. The *in vitro* screening of the novel compounds in the MTT test revealed their very high cytotoxic activity in the low micromolar range in HL-60 and MCF-7 cells. An interesting observation was that in both tested cancer cell lines *N,O-syn* 3-diethoxyphosphorylfuroquinoline-4,9-diones were more cytotoxic than the respective *N,O-anti* regioisomers. The comparison of the cytotoxic activity of 3-diethoxyphosphorylfuroquinoline-4,9-diones **9** and **10** with formerly published 3-diethoxyphosphorylnaphthofuran-4,9-diones showed that analogs containing a nitrogen atom were 15- to 30-fold more active in HL-60 cells and 2- to 5-fold more active in MCF-7 cells.

Among novel analogs, compounds **9c** and **9i** had the most favorable cancer/healthy cells cytotoxicity ratio and their activity in HL-60 cells was further evaluated. Both these analogs showed similar mode of action, significantly inducing the S-phase cell cycle arrest, reducing cell proliferation, promoting DNA damage and apoptosis. It could be speculated that the decreased proliferation and mitochondria-dependent apoptosis in HL-60 cells induced by **9c** and **9i** were associated with the enhanced intracellular ROS generation and NQO1 depletion. The results suggest, that the novel furoquinoline-4,9-dione analogs may be further developed as a potential anti-cancer treatment.

4. Experimental

4.1. General methods

Analytical grade solvents and commercially available reagents were used without further purification. NMR spectra were recorded on a Bruker UltraShield 700 instrument, running at 700 MHz for ^{1}H, and 176 MHz for ^{13}C and 283 MHz for ^{31}P. Chemical shifts (δ) are reported in ppm relative to residual solvent signals ($CDCl_3$: 7.26 ppm for ^{1}H NMR, 77.16 ppm for ^{13}C NMR). Mass spectra were obtained on a Bruker Maxis Impact spectrometer using electrospray (ES+) ionization (referenced to the mass of the charged species). Thin-layer chromatography was performed with precoated TLC sheets of silica gel 60 F254 (Aldrich®) and visualized by ultraviolet irradiation. Silica gel (silica gel 60, 230–400 mesh, Aldrich®) was used for column chromatography.

4.2. General procedure for the synthesis of 3-diethoxyphosphorylfuroquinoline-4,9-diones ***9a-i*** and ***10a-i***

A mixture of 6,7-dichloroquinoline-5,8-dione **7** (0.91 g, 4.0 mmol) K_2CO_3 (1.66 g, 12.0 mmol) and corresponding diethyl acylmethylphosphonate **8** (4.0 mmol) in MeCN (50 mL) was stirred

at 65 °C for 18 h. The reaction mixture was poured into cold water (50 mL). Extraction with EtOAc (3 × 50 mL), drying ($MgSO_4$) and evaporation of the solvent gave the crude product, which was purified by column chromatography [EtOAc].

Diethyl (2-methyl-4,9-dioxo-4,9-dihydrofuro[3,2-g]quinolin-3-yl*) phosphonate (**9a**):* yellow solid, mp 190–192 °C; ^{1}H NMR (700 MHz, $CDCl_3$) δ 9.02 (dd, *J* = 4.6, 1.7 Hz, 1H), 8.50 (dd, *J* = 7.9, 1.7 Hz, 1H), 7.69 (dd, *J* = 7.9, 4.6 Hz, 1H), 4.29 (ddq, *J* = 10.1, 8.4, 7.1 Hz, 2H), 4.21 (ddq, *J* = 10.1, 8.6, 7.1 Hz, 2H), 2.80 (d, *J* = 2.0 Hz, 3H), 1.35 (t, *J* = 7.1 Hz, 6H). ^{13}C NMR (176 MHz, $CDCl_3$) δ 177.79, 171.47, 168.85 (d, *J* = 26.1 Hz), 154.47, 152.41 (d, *J* = 11.8 Hz), 147.89, 135.37, 130.50 (d, *J* = 9.6 Hz), 130.37, 127.67, 107.96 (d, *J* = 214.7 Hz), 63.01 (d, *J* = 5.7 Hz), 16.45 (d, *J* = 6.4 Hz), 14.60. ^{31}P NMR (283 MHz, $CDCl_3$) δ 8.41; HRMS *m*/*z*, calcd [M+H]+ 350.0793, observed 350.0796.

Diethyl (2-methyl-4,9-dioxo-4,9-dihydrofuro[2,3-g]quinolin-3-yl*) phosphonate (**10a**):* yellow solid, mp 110–112 °C; ^{1}H NMR (700 MHz, $CDCl_3$) δ 9.03 (dd, *J* = 4.7, 1.8 Hz, 1H), 8.52 (dd, *J* = 7.9, 1.8 Hz, 1H), 7.69 (dd, *J* = 7.9, 4.7 Hz, 1H), 4.37–4.29 (m, 2H), 4.29–4.21 (m, 2H), 2.82 (d, *J* = 2.1 Hz, 3H), 1.35 (t, *J* = 7.1 Hz, 6H). ^{13}C NMR (176 MHz, $CDCl_3$) δ 177.01, 172.35, 168.90 (d, *J* = 26.6 Hz), 154.47, 151.43 (d, *J* = 11.7 Hz), 148.91, 134.84, 131.20 (d, *J* = 9.7 Hz), 128.77, 127.49, 108.49 (d, *J* = 215.2 Hz), 63.25 (d, *J* = 6.1 Hz), 16.46 (d, *J* = 6.6 Hz), 14.60. ^{31}P NMR (283 MHz, $CDCl_3$) δ 7.67. HRMS *m*/*z*, calcd [M+H]+ 350.0793, observed 350.0797.

Diethyl (4,9-dioxo-2-phenyl-4,9-dihydrofuro[3,2-g]quinolin-3-yl*) phosphonate (**9b**):* orange solid, mp 146–148 °C; ^{1}H NMR (700 MHz, $CDCl_3$) δ 9.03 (dd, *J* = 4.6, 1.7 Hz, 1H), 8.54 (dd, *J* = 7.9, 1.7 Hz, 1H), 7.88–7.84 (m, 2H), 7.71 (dd, *J* = 7.9, 4.6 Hz, 1H), 7.55–7.50 (m, 1H), 7.50–7.45 (m, 2H), 4.19 (ddq, *J* = 10.1, 7.2, 7.1 Hz, 2H), 4.10 (ddq, *J* = 10.1, 8.7, 7.1 Hz, 2H), 1.18 (t, *J* = 7.1 Hz, 6H).; ^{13}C NMR (176 MHz, $CDCl_3$) δ 177.74, 171.60, 166.00 (d, *J* = 23.5 Hz), 154.47, 152.68 (d, *J* = 12.5 Hz), 147.85, 135.47, 131.87 (d, *J* = 10.1 Hz), 131.56, 130.58, 130.35, 128.25, 127.78, 127.76, 108.20 (d, *J* = 213.8 Hz), 63.14 (d, *J* = 6.0 Hz), 16.16 (d, *J* = 6.8 Hz). ^{31}P NMR (283 MHz, $CDCl_3$) δ 7.40; HRMS *m*/*z*, calcd [M+H]+ 412.0950, observed 412.0965.

Diethyl (4,9-dioxo-2-phenyl-4,9-dihydrofuro[2,3-g]quinolin-3-yl*) phosphonate (**10b**):* yellow solid, mp 134–136 °C; ^{1}H NMR (700 MHz, $CDCl_3$) δ 9.04 (dd, *J* = 4.6, 1.8 Hz, 1H), 8.53 (dd, *J* = 7.8, 1.8 Hz, 1H), 7.91–7.87 (m, 2H), 7.69 (dd, *J* = 7.8, 4.6 Hz, 1H), 7.54–7.50 (m, 1H), 7.50–7.45 (m, 2H), 4.27–4.21 (m, 2H), 4.21–4.14 (m, 2H), 1.20 (t, *J* = 7.1 Hz, 6H). ^{13}C NMR (176 MHz, $CDCl_3$) δ 176.95, 172.47, 166.06 (d, *J* = 23.6 Hz), 154.54, 151.69 (d, *J* = 12.1 Hz), 149.04, 134.78, 132.40 (d, *J* = 10.0 Hz), 131.51, 130.32, 128.77, 128.27, 127.87, 127.49, 108.81 (d, *J* = 214.8 Hz), 63.35 (d, *J* = 6.3 Hz), 16.23 (d, *J* = 6.8 Hz). ^{31}P NMR (283 MHz, $CDCl_3$) δ 7.16. HRMS *m*/*z*, calcd [M+H]+ 412.0950, observed 412.0957.

Diethyl (2-(4-methoxyphenyl)-4,9-dioxo-4,9-dihydrofuro[3,2-g] quinolin-3-yl*)phosphonate (**9c**):* orange solid, mp 208–210 °C; ^{1}H NMR (700 MHz, $CDCl_3$) δ 9.04 (dd, *J* = 4.6, 1.8 Hz, 1H), 8.53 (dd, *J* = 7.9, 1.7 Hz, 1H), 7.91–7.87 (m, 2H), 7.70 (dd, *J* = 7.9, 4.6 Hz, 1H), 7.01–6.96 (m, 2H), 4.26–4.17 (m, 2H), 4.17–4.09 (m, 2H), 3.87 (s, 3H), 1.23 (t, *J* = 7.1 Hz, 6H). ^{13}C NMR (176 MHz, $CDCl_3$) δ 177.82, 171.53, 166.34 (d, *J* = 23.8 Hz), 162.41, 154.43, 152.36 (d, *J* = 12.2 Hz), 147.97, 135.44, 132.15 (d, *J* = 10.1 Hz), 132.14, 130.63, 127.66, 120.09, 113.82, 106.69 (d, *J* = 213.6 Hz), 63.08 (d, *J* = 5.8 Hz), 55.59, 16.29 (d, *J* = 6.6 Hz). ^{31}P NMR (283 MHz, $CDCl_3$) δ 7.94. HRMS *m*/*z*, calcd [M+H]+ 442.1056, observed 442.1059.

Diethyl (2-(4-methoxyphenyl)-4,9-dioxo-4,9-dihydrofuro[2,3-g] quinolin-3-yl*)phosphonate (**10c**):* yellow solid, mp 156–158 °C; ^{1}H NMR (700 MHz, $CDCl_3$) δ 9.04 (dd, *J* = 4.7, 1.7 Hz, 1H), 8.53 (dd, *J* = 7.8, 1.7 Hz, 1H), 7.94–7.89 (m, 2H), 7.69 (dd, *J* = 7.8, 4.7 Hz, 1H), 7.01–6.97 (m, 2H), 4.28–4.22 (m, 2H), 4.22–4.16 (m, 2H), 3.86 (s, 3H), 1.25 (t, *J* = 7.1 Hz, 6H). ^{13}C NMR (176 MHz, $CDCl_3$) δ 177.02, 172.38, 166.40 (d, *J* = 24.6 Hz), 162.38, 154.45, 151.33 (d, *J* = 12.2 Hz), 149.12, 134.74, 132.70 (d, *J* = 9.7 Hz), 132.10, 128.83, 127.44, 120.17, 113.83, 107.29 (d, *J* = 214.9 Hz), 63.30 (d, *J* = 6.3 Hz), 55.58, 16.34 (d, *J* = 6.5 Hz). ^{31}P NMR (283 MHz, $CDCl_3$) δ 7.63. HRMS *m*/*z*, calcd [M+H]+ 442.1056, observed 442.1066.

Diethyl (4,9-dioxo-2-(3,4,5-trimethoxyphenyl)-4,9-dihydrofuro [3,2-g]quinolin-3-yl*)phosphonate (**9d**):* red solid, mp 186–188 °C; ^{1}H NMR (700 MHz, $CDCl_3$) δ 9.05 (dd, *J* = 4.6, 1.7 Hz, 1H), 8.54 (dd, *J* = 7.9, 1.7 Hz, 1H), 7.71 (dd, *J* = 7.9, 4.6 Hz, 1H), 7.24 (s, 2H), 4.26–4.18 (m, 2H), 4.18–4.11 (m, 2H), 3.94 (s, 6H), 3.91 (s, 3H), 1.23 (t, *J* = 7.1 Hz, 6H). ^{13}C NMR (176 MHz, $CDCl_3$) δ 177.69, 171.55, 165.87 (d, *J* = 23.6 Hz), 154.50, 153.00, 152.35 (d, *J* = 12.1 Hz), 147.86, 141.24, 135.50, 132.15 (d, *J* = 10.1 Hz), 130.64, 127.77, 122.59, 107.86, 107.62 (d, *J* = 213.0 Hz), 63.16 (d, *J* = 5.8 Hz), 61.13, 56.55, 16.28 (d, *J* = 6.6 Hz). ^{31}P NMR (283 MHz, $CDCl_3$) δ 7.86. HRMS *m*/*z*, calcd [M+H]+ 502.1267, observed 502.1288.

Diethyl (4,9-dioxo-2-(3,4,5-trimethoxyphenyl)-4,9-dihydrofuro [2,3-g]quinolin-3-yl*)phosphonate (**10d**):* orange solid, mp 168–170 °C; ^{1}H NMR (700 MHz, $CDCl_3$) δ 9.05 (dd, *J* = 4.6, 1.7 Hz, 1H), 8.54 (dd, *J* = 7.8, 1.7 Hz, 1H), 7.70 (dd, *J* = 7.8, 4.6 Hz, 1H), 7.28 (s, 2H), 4.30–4.24 (m, 2H), 4.24–4.18 (m, 2H), 3.94 (s, 6H), 3.91 (s, 3H), 1.25 (t, *J* = 7.1 Hz, 6H). ^{13}C NMR (176 MHz, $CDCl_3$) δ 176.90, 172.43, 165.91 (d, *J* = 24.1 Hz), 154.57, 153.02, 151.33 (d, *J* = 12.1 Hz), 149.11, 141.19, 134.78, 132.65 (d, *J* = 9.6 Hz), 128.75, 127.51, 122.71, 108.27 (d, *J* = 214.2 Hz), 107.82, 63.37 (d, *J* = 6.3 Hz), 61.11, 56.56, 16.33 (d, *J* = 6.9 Hz). ^{31}P NMR (283 MHz, $CDCl_3$) δ 7.64. HRMS *m*/*z*, calcd [M+H]+ 502.1267, observed 502.1268.

Diethyl (2-(benzo[d] [1,3]*dioxol*-5-yl*)-4,9-dioxo-4,9-dihydrofuro [3,2-g]quinolin*-3-yl*)phosphonate (**9e**):* red solid, mp 122–124 °C; ^{1}H NMR (700 MHz, $CDCl_3$) δ 9.05 (dd, *J* = 4.6, 1.7 Hz, 1H), 8.54 (dd, *J* = 7.9, 1.7 Hz, 1H), 7.71 (dd, *J* = 7.9, 4.6 Hz, 1H), 7.49 (dd, *J* = 8.1, 1.8 Hz, 1H), 7.40 (d, *J* = 1.8 Hz, 1H), 6.91 (d, *J* = 8.1 Hz, 1H), 6.06 (s, 2H), 4.24 (ddq, *J* = 10.1, 7.8, 7.1 Hz, 2H), 4.16 (ddq, *J* = 10.1, 8.8, 7.1 Hz, 2H), 1.26 (t, *J* = 7.1 Hz, 6H). ^{13}C NMR (176 MHz, $CDCl_3$) δ 177.77, 171.54, 165.84 (d, *J* = 24.0 Hz), 154.48, 152.32 (d, *J* = 12.2 Hz), 150.65, 147.92, 147.68, 135.49, 132.04 (d, *J* = 10.1 Hz), 130.63, 127.73, 125.91, 121.34, 110.35, 108.32, 107.14 (d, *J* = 213.6 Hz), 101.98, 63.16 (d, *J* = 5.8 Hz), 16.32 (d, *J* = 6.8 Hz). ^{31}P NMR (283 MHz, $CDCl_3$) δ 7.71. HRMS *m*/*z*, calcd [M+H]+ 456.0848, observed 456.0863.

Diethyl (2-(benzo[d] [1,3]*dioxol*-5-yl*)-4,9-dioxo-4,9-dihydrofuro [2,3-g]quinolin*-3-yl*)phosphonate (**10e**):* orange solid, mp 180–182 °C; ^{1}H NMR (700 MHz, $CDCl_3$) δ 9.06 (dd, *J* = 4.6, 1.7 Hz, 1H), 8.55 (dd, *J* = 7.8, 1.7 Hz, 1H), 7.70 (dd, *J* = 7.8, 4.6 Hz, 1H), 7.53 (dd, *J* = 8.1, 1.8 Hz, 1H), 7.43 (d, *J* = 1.8 Hz, 1H), 6.92 (d, *J* = 8.1 Hz, 1H), 6.06 (s, 2H), 4.28 (ddq, *J* = 10.1, 7.8, 7.1 Hz, 2H), 4.22 (ddq, *J* = 10.1, 8.8, 7.1 Hz, 2H), 1.28 (t, *J* = 7.1 Hz, 6H). ^{13}C NMR (176 MHz, $CDCl_3$) δ 176.98, 172.42, 165.93 (d, *J* = 24.2 Hz), 154.54, 151.32 (d, *J* = 12.1 Hz), 150.63, 149.13, 147.71, 134.80, 132.60 (d, *J* = 9.9 Hz), 128.83, 127.50, 125.93, 121.44, 110.32, 108.35, 107.77 (d, *J* = 214.7 Hz), 101.97, 63.39 (d, *J* = 6.3 Hz), 16.39 (d, *J* = 6.7 Hz). ^{31}P NMR (283 MHz, $CDCl_3$) δ 7.40. HRMS *m*/*z*, calcd [M+H]+ 456.0848, observed 456.0854.

Diethyl (2-(4-nitrophenyl)-4,9-dioxo-4,9-dihydrofuro[3,2-g]quinolin-3-yl*)phosphonate (**9f**):* yellow solid, mp 162–164 °C; ^{1}H NMR (700 MHz, $CDCl_3$) δ 9.09 (dd, *J* = 4.6, 1.7 Hz, 1H), 8.58 (dd, *J* = 7.9, 1.7 Hz, 1H), 8.37–8.33 (m, 2H), 8.18–8.14 (m, 2H), 7.75 (dd, *J* = 7.9, 4.6 Hz, 1H), 4.29 (ddq, *J* = 10.2, 8.0, 7.1 Hz, 2H), 4.20 (ddq, *J* = 10.2, 8.9, 7.1 Hz, 2H), 1.28 (t, *J* = 7.1 Hz, 6H). ^{13}C NMR (176 MHz, $CDCl_3$) δ 177.42, 171.65, 163.02 (d, *J* = 23.7 Hz), 154.76, 153.28 (d, *J* = 12.0 Hz), 149.37, 147.76, 135.66, 133.59, 131.56, 131.42 (d, *J* = 9.1 Hz), 130.64, 128.03, 123.38, 110.72 (d, *J* = 212.0 Hz), 63.53 (d, *J* = 5.9 Hz), 16.38 (d, *J* = 6.4 Hz). ^{31}P NMR (283 MHz, $CDCl_3$) δ 7.27. HRMS *m*/*z*, calcd [M+H]+ 457.0801, observed 457.0802.

Diethyl (2-(4-nitrophenyl)-4,9-dioxo-4,9-dihydrofuro[2,3-g]quinolin-3-yl*)phosphonate (**10f**):* yellow solid, mp 212–214 °C; ^{1}H NMR (700 MHz, $CDCl_3$) δ 9.05 (dd, *J* = 4.6, 1.8 Hz, 1H), 8.53 (dd, *J* = 7.8, 1.7 Hz, 1H), 7.96–7.92 (m, 2H), 7.70 (dd, *J* = 7.8, 4.7 Hz, 1H), 7.17 (dd,

J = 9.5, 7.7 Hz, 2H), 4.30–4.23 (m, 2H), 4.20 (ddq, J = 10.1, 8.7, 7.1 Hz, 2H), 1.24 (t, J = 7.0 Hz, 6H). ^{13}C NMR (176 MHz, $CDCl_3$) δ 176.61, 172.56, 163.07 (d, J = 24.0 Hz), 154.89, 152.33 (d, J = 12.0 Hz), 149.34, 148.98, 134.97, 133.64, 131.94 (d, J = 9.2 Hz), 131.52, 128.75, 127.72, 123.38, 111.25 (d, J = 212.4 Hz), 63.74 (d, J = 6.3 Hz), 16.39 (d, J = 6.6 Hz). ^{31}P NMR (283 MHz, $CDCl_3$) δ 5.88. HRMS *m/z*, calcd [M+H]+ 457.0801, observed 457.0803.

Diethyl (2-(4-fluorophenyl)-4,9-dioxo-4,9-dihydrofuro[3,2-g]quinolin-3-yl)*phosphonate (**9g**):* yellow solid, mp 148–150 °C; ^{1}H NMR (700 MHz, $CDCl_3$) δ 9.04 (dd, J = 4.6, 1.7 Hz, 1H), 8.54 (dd, J = 7.9, 1.7 Hz, 1H), 7.94–7.89 (m, 2H), 7.71 (dd, J = 7.9, 4.6 Hz, 1H), 7.20–7.14 (m, 2H), 4.22 (ddq, J = 10.1, 8.1, 7.2 Hz, 2H), 4.14 (ddq, J = 10.1, 8.7, 7.1 Hz, 2H), 1.23 (t, J = 7.1 Hz, 6H). ^{13}C NMR (176 MHz, $CDCl_3$) δ 177.65, 171.58, 164.99 (d, J = 23.9 Hz), 164.71 (d, J = 253.7 Hz), 154.52, 152.63 (d, J = 12.1 Hz), 147.81, 135.49, 132.69 (d, J = 8.8 Hz), 131.74 (d, J = 10.0 Hz), 130.57, 127.80, 123.96 (d, J = 3.6 Hz), 115.60 (d, J = 22.2 Hz), 108.13 (d, J = 213.1 Hz), 63.20 (d, J = 5.8 Hz), 16.26 (d, J = 6.8 Hz). ^{31}P NMR (283 MHz, $CDCl_3$) δ 7.27. HRMS *m/z*, calcd [M+H]+ 430.0856, observed 430.0865.

Diethyl (2-(4-fluorophenyl)-4,9-dioxo-4,9-dihydrofuro[2,3-g]quinolin-3-yl)*phosphonate (**10g**):* yellow solid, mp 130–132 °C; ^{1}H NMR (700 MHz, $CDCl_3$) δ 9.05 (dd, J = 4.6, 1.8 Hz, 1H), 8.53 (dd, J = 7.8, 1.8 Hz, 1H), 7.96–7.92 (m, 2H), 7.70 (dd, J = 7.8, 4.6 Hz, 1H), 7.20–7.15 (m, 2H), 4.30–4.23 (m, 2H), 4.20 (ddq, J = 10.1, 8.7, 7.1 Hz, 2H), 1.24 (t, J = 7.1 Hz, 6H). ^{13}C NMR (176 MHz, $CDCl_3$) δ 176.87, 172.46, 165.07 (d, J = 24.2 Hz), 164.71 (d, J = 253.6 Hz), 154.60, 151.65 (d, J = 12.2 Hz), 149.01, 134.81, 132.67 (d, J = 8.9 Hz), 132.29 (d, J = 9.6 Hz), 128.74, 127.54, 124.03 (d, J = 3.3 Hz), 115.61 (d, J = 22.2 Hz), 108.70 (d, J = 214.2 Hz), 63.43 (d, J = 6.1 Hz), 16.31 (d, J = 6.5 Hz). ^{31}P NMR (283 MHz, $CDCl_3$) δ 6.97. HRMS *m/z*, calcd [M+H]+ 430.0856, observed 430.0860.

Diethyl (2-(4-chlorophenyl)-4,9-dioxo-4,9-dihydrofuro[3,2-g]quinolin-3-yl)*phosphonate (**9h**):* yellow solid, mp 94–96 °C; ^{1}H NMR (700 MHz, $CDCl_3$) δ 9.05 (dd, J = 4.6, 1.7 Hz, 1H), 8.55 (dd, J = 7.9, 1.7 Hz, 1H), 7.90–7.85 (m, 2H), 7.72 (dd, J = 7.9, 4.6 Hz, 1H), 7.49–7.45 (m, 2H), 4.28–4.20 (m, 2H), 4.16 (ddq, J = 10.1, 8.8, 7.1 Hz, 2H), 1.25 (t, J = 7.1 Hz, 6H). ^{13}C NMR (176 MHz, $CDCl_3$) δ 177.63, 171.60, 164.82 (d, J = 23.6 Hz), 154.57, 152.77 (d, J = 12.3 Hz), 147.86, 138.08, 135.53, 131.74 (d, J = 10.1 Hz), 131.70, 130.62, 128.67, 127.82, 126.23, 108.64 (d, J = 212.9 Hz), 63.28 (d, J = 5.8 Hz), 16.30 (d, J = 6.5 Hz). ^{31}P NMR (283 MHz, $CDCl_3$) δ 7.12. HRMS *m/z*, calcd [M+H]+ 446.0560, observed 446.0567.

Diethyl (2-(4-chlorophenyl)-4,9-dioxo-4,9-dihydrofuro[2,3-g]quinolin-3-yl)*phosphonate (**10h**):* yellow solid, mp 144–146 °C; ^{1}H NMR (700 MHz, $CDCl_3$) δ 9.07 (dd, J = 4.6, 1.7 Hz, 1H), 8.55 (dd, J = 7.8, 1.7 Hz, 1H), 7.92–7.88 (m, 2H), 7.71 (dd, J = 7.8, 4.6 Hz, 1H), 7.49–7.45 (m, 2H), 4.28 (ddq, J = 10.1, 8.0, 7.1 Hz, 2H), 4.22 (ddq, J = 10.1, 8.8, 7.1 Hz, 2H), 1.26 (t, J = 7.1 Hz, 6H). ^{13}C NMR (176 MHz, $CDCl_3$) δ 176.83, 172.49, 164.90 (d, J = 24.2 Hz), 154.66, 151.79 (d, J = 12.2 Hz), 149.07, 138.04, 134.85, 132.30 (d, J = 9.5 Hz), 131.68, 128.79, 128.68, 127.56, 126.31, 109.22 (d, J = 213.6 Hz), 63.50 (d, J = 6.0 Hz), 16.35 (d, J = 6.4 Hz). ^{31}P NMR (283 MHz, $CDCl_3$) δ 6.79. HRMS *m/z*, calcd [M+H]+ 446.0560, observed 446.0566.

Diethyl (2-(2-chlorophenyl)-4,9-dioxo-4,9-dihydrofuro[3,2-g]quinolin-3-yl)*phosphonate (**9i**):* brown solid, mp 140–142 °C; ^{1}H NMR (700 MHz, $CDCl_3$) δ 9.05 (dd, J = 4.7, 1.7 Hz, 1H), 8.56 (dd, J = 7.9, 1.7 Hz, 1H), 7.72 (dd, J = 7.9, 4.7 Hz, 1H), 7.52–7.45 (m, 3H), 7.40–7.35 (m, 1H), 4.19 (ddq, J = 10.1, 8.0, 7.1 Hz, 2H), 4.08 (ddq, J = 10.1, 8.8, 7.1 Hz, 2H), 1.14 (t, J = 7.1 Hz, 6H). ^{13}C NMR (176 MHz, $CDCl_3$) δ 177.77, 171.71, 162.92 (d, J = 21.8 Hz), 154.59, 153.18 (d, J = 12.0 Hz), 147.92, 135.48, 134.81, 132.65, 132.33, 130.66 (d, J = 10.2 Hz), 130.48, 129.71, 128.22, 127.85, 126.50, 111.91 (d, J = 215.3 Hz), 63.11 (d, J = 6.1 Hz), 16.17 (d, J = 6.9 Hz). ^{31}P NMR (283 MHz, $CDCl_3$) δ 6.16. HRMS *m/z*, calcd [M+H]+ 446.0560, observed 446.0567.

Diethyl (2-(2-chlorophenyl)-4,9-dioxo-4,9-dihydrofuro[2,3-g]quinolin-3-yl)*phosphonate (**10i**):* brown solid, mp 170–172 °C; ^{1}H NMR (700 MHz, $CDCl_3$) δ 9.05 (dd, J = 4.7, 1.7 Hz, 1H), 8.54 (dd, J = 7.8, 1.7 Hz, 1H), 7.70 (dd, J = 7.8, 4.7 Hz, 1H), 7.53–7.44 (m, 3H), 7.39–7.34 (m, 1H), 4.22 (ddq, J = 10.1, 8.1, 7.1 Hz, 2H), 4.13 (ddq, J = 10.1, 8.9, 7.1 Hz, 2H), 1.15 (t, J = 6.8 Hz, 6H). ^{13}C NMR (176 MHz, $CDCl_3$) δ 176.95, 172.57, 162.97 (d, J = 22.3 Hz), 154.64, 152.20 (d, J = 12.1 Hz), 148.90, 134.88, 134.72, 132.75, 132.27, 131.23 (d, J = 10.2 Hz), 129.68, 128.85, 128.22, 127.55, 126.48, 112.41 (d, J = 215.7 Hz), 63.30 (d, J = 6.1 Hz), 16.20 (d, J = 6.9 Hz). ^{31}P NMR (283 MHz, $CDCl_3$) δ 5.83. HRMS *m/z*, calcd [M+H]+ 446.0560, observed 446.0563.

4.3. Biological tests

4.3.1. Cell cultures and sample preparations

HL-60 and MCF-7 cell lines were purchased from the European Collection of Cell Cultures (ECACC). Leukemia cells were cultured in RPMI 1640 plus GlutaMax I medium (Invitrogen, Grand Island, NY, USA), supplemented with 10% heat-inactivated FBS (Biological Industries, Beit-Haemek, Israel) and antibiotics (100 μg/mL streptomycin and 100 U/mL penicillin) (Sigma-Aldrich**,** St. Louis, MO, USA). MCF-7 cells were cultured in Minimum Essential Medium Eagle (MEME, Sigma-Aldrich**,** St. Louis, MO, USA) supplemented with 10% heat-inactivated fetal bovine serum (FBS) (Biological Industries, Beit-Haemek, Israel), 2 mM glutamine, Men Non-essential amino acid solution and antibiotics (100 μg/mL streptomycin and 100 U/mL penicillin), all from Sigma-Aldrich (Sigma-Aldrich, St. Louis, MO, USA). HUVEC and MCF-10 A were purchased from the American Type Culture Collection (ATCC). HUVEC cells were cultured using EGM-2 Endothelial Medium BulletKit, both purchased from Lonza (Lonza, Walkersville, MD, USA). For MCF-10 A cells MEGM Mammary Epithelial BulletKit was used. Cells were maintained at 37 °C in a 5% CO_2 atmosphere and grown until 80% confluent.

For biological experiments the compounds were dissolved in DMSO (Sigma-Aldrich, Louis, MO, USA) and further diluted in culture medium to obtain less than 0.1% DMSO concentration. In each experiment controls without and with DMSO were performed. DMSO in 0.1% concentration had no effects on the observed parameters.

4.3.2. Metabolic activity by MTT assay

The MTT (3-(4,5-dimethyldiazol-2-yl)-2,5 diphenyl tetrazolium bromide) assay was performed according to Mossman [39]. In brief, exponentially growing cells (HL-60, MCF-7, HUVEC, MCF-10 A) were seeded in 24-well plates at a density of 8×10^4/mL and left to grow for 24 h. The cells treated with various concentrations of the tested analogs were incubated for 24 h or 48 h. Then, MTT solution (100 μL; 5 mg/mL in PBS) was added to each well. Following 1.5 h of incubation, the plates were centrifuged and the supernatant was discarded. DMSO (1 mL) was added to each well to dissolve the formazan crystals. The absorbance was measured at 560 nm using FlexStation 3 Multi-Mode Microplate Reader (Molecular Devices, LLC,CA, USA) and compared with control (untreated cells). Assays were performed twice in triplicate for each compound. The IC_{50} values were calculated from concentration–response curves.

4.3.3. Apoptosis, DNA damage and cell proliferation assay

The cell-cycle distribution, cell proliferation, apoptosis and DNA damage were assessed using Apoptosis, DNA Damage and Cell Proliferation Kit (BD Biosciences, San Jose, CA, USA). In brief, 2.0×10^5/mL HL-60 cells were seeded in 6-well plates and cultured for 24 h. Then, the cells were treated with various concentrations of **9i** and **9c**. Cells incubated without tested compound were used as a control. Following 24 h incubation, cells were treated with BrdU solution (10 μM final concentration)for 8 h and collected by

centrifugation. Then, the cells were fixed, permeabilized and incubated with DNase (300 μg/mL in PBS) for 1 h at 37 °C. Afterwards, the cells were stained with Anti-BrdU, Anti-H2AX (pS139) and Anti-Cleaved PARP (Asp214) fluorescent antibodies for 20 min, in the dark at room temperature. For cell cycle analysis, total DNA was stained with DAPI solution (1 μg/mL in staining buffer). Cells were analyzed by flow cytometry using CytoFLEX (Beckman Coulter, Inc). The data was analyzed using Kaluza Analysis Software v2 (Beckman Coulter, Inc).

4.3.4. Apoptosis detection by Annexin V and Propidium iodide staining

Induction of apoptosis was determined using FITC Annexin V Apoptosis Detection Kit I (BD Biosciences, San Jose, CA, USA). Briefly, 2.0×10^5/mL HL-60 cells were plated in 6-well plates, cultured overnight and treated with various concentrations of **9i** and **9c** for 24 h or untreated for control. The cells were then collected by centrifugation, washed with PBS, resuspended in 1x binding buffer and stained with FITC Annexin V and Propidium Iodide at room temperature for 15 min in the dark. The percentage of apoptotic cells was assessed by flow cytometry using CytoFLEX (Beckman Coulter, Inc., Brea, CA, USA). Data analysis was performed using Kaluza Analysis Software v2 (Beckman Coulter, Inc., Indianapolis, IN, USA).

4.3.5. ROS detection

The CellROX Oxidative Stress Green Reagent (LifeTechnologies, Carlsbad, CA, USA) was used to detect changes of ROS. HL-60 cells were plated in a 24-well plate, cultured overnight and then treated with IC_{50} concentrations of **9i** and **9c** for 24 h. Afterwards, the CellROX Green Reagent was added to each well and incubated for 30 min at 37 °C. The cells were then washed with PBS and analyzed by flow cytometry using CytoFLEX (Beckman Coulter, Inc). Data analysis was performed using Kaluza Analysis Software v2 (Beckman Coulter, Inc).

4.3.6. Mitochondrial membrane potential assay

The changes in the mitochondrial membrane potential were evaluated with Flow Cytometry Mitochondrial Membrane Potential Detection Kit (BD Biosciences, San Jose, CA, USA). HL-60 cells were plated in 6-well plates at a density 2×10^5/mL. After 24 h incubation, the cells were treated with various concentrations of **9i** and **9c** or not treated for control for 24 h. Cells treated with FCCP (carbonilcyanide ptriflouromethoxyphenylhydrazone, 30 μM) for 30 min at 37 °C were used as a positive control. Subsequently, cells were collected by centrifugation and incubated for 15 m in with JC-1 Solution (1st J-aggregate-forming cationic dye).Finally, the cells were washed twice and resuspended in Assay Buffer and analyzed by flowcytometry using CytoFLEX (Beckman Coulter, Inc). Data analysis was performed using Kaluza Analysis Software v2 (Beckman Coulter, Inc).

4.3.7. NQO1 activity assay

The effect of **9i** and **9c** treatment on NQO1 activity in HL-60 cells was determined using NQO1 activity assay kit (Abcam, Cambridge, MA, USA). Briefly, HL-60 cells treated with various concentrations of **9i** and **9c** for 24 h were collected by centrifugation and the cell pellet was solubilized in extraction buffer on ice. After centrifugation (18,000×*g*, 20 min, 4 °C), supernatants were transferred into clean tubes and the protein concentration was quantified using Quick Start™ Bradford Protein Assay Kit (Bio-Rad Laboratories, Hercules, California, United States). Samples were diluted with supplemented buffer to 2x the required final concentration. For each sample, two wells were used – for the activity assessment with and without inhibitor – in duplicate. Absorbance was measured at 440 nm for 5 min with 20 s interval and shaking before and between readings using FlexStation 3 Multi-Mode Microplate Reader (Molecular Devices, LLC,CA, USA). NQO1 activity is expressed as the change in absorbance/min/amount of sample loaded into the well.

4.3.8. Statistical analysis

Data are expressed as mean ± SEM. Assays were performed in triplicate. Statistical analyses were performed using Prism 6.0 (GraphPad Software Inc., San Diego, CA, USA). Statistical significance was assessed using Student's t-test (for comparisons of two groups) or one-way ANOVA followed by a post-hoc multiple comparison Student-Newman-Keuls test (for comparisons of three or more groups).*$p < 0.05$, **$p < 0.01$, and ***$p < 0.001$ were considered significant.

Declaration of competing interest

The authors declare that they have no known competing financial interests or personal relationships that could have appeared to influence the work reported in this paper.

Acknowledgements

This study was supported financially by the grant from the Medical University of Lodz No. 503/1-156-02/503-11-001-19-00 and from Lodz University of Technology No. 501-3-32-1-2.

Appendix A. Supplementary data

Supplementary data to this article can be found online at https://doi.org/10.1016/j.ejmech.2021.113429.

References

[1] J.A. Joule, K. Mills, Heterocyclic Chemistry, Blackwell Science, Oxford, 2000.
[2] D.K. Lang, R. Kaur, R. Arora, B. Saini, S. Arora, Nitrogen-containing heterocycles as anticancer agents: an overview, Anticancer Agents Med. Chem. 20 (2020) 2150–2168.
[3] N. Kerru, L. Gummidi, S. Maddila, K.K. Gangu, S.B. Jonnalagadda, A Review on recent advances in nitrogen-containing molecules and their biological applications, Molecules 25 (2020) 1909.
[4] M. Behforouz, J. Haddad, W. Cai, Z. Gu, Chemistry of quinoline-5,8-diones, J. Org. Chem. 63 (1998) 343–346.
[5] Ch.-K. Ryu, I.-K. Lee, S.-H. Jung, Ch.-O. Lee, Synthesis and cytotoxic activities of 6-chloro-7-arylamino-5,8-isoquinolinediones, Bioorg. Med. Chem. Lett 9 (1999) 1075–1080.
[6] M. Kadela-Tomanek, E. Bębenek, E. Chrobak, S. Boryczka, 5,8-Quinolinedione scaffold as a promising moiety of bioactive agents, Molecules 24 (2019) 4115–4135.
[7] J.W. Lown, S.-K. Sim, Studies related to antitumor antibiotics. Part VII. Synthesis of streptonigrin analogues and their single strand scission of DNA, Can. J. Chem. 54 (1976) 2563–2572.
[8] C.F.C. Lam, A.N. Pearce, S.H. Tan, M. Kaiser, B.R. Copp, Discovery and evaluation of thiazinoquinones as anti-protozoal agents, Mar. Drugs 11 (2013) 3472–3499.
[9] H.-K. Rhee, H.J. Park, S.K. Lee, Ch.-O. Lee, H.-Y.P. Choo, Synthesis, cytotoxicity, and DNA topoisomerase II inhibitory activity of benzofuroquinolinediones, Bioorg. Med. Chem. 15 (2007) 1651–1658.
[10] H. Ban, S. Kamioka, T. Furuta, H. Kitano, Ch. J. Li, New Tricyclic Quinone Derivative, US patent US 2017/0015677 A1.
[11] L.-M. Yu, Z. Hu, Y. Chen, A. Ravji, S. Lopez, C.B. Plescia, Q. Yu, H. Yang, M. Abdelmalak, S. Saha, K. Agama, E. Kiselev, Ch. Marchand, Y. Pommier, L.-K. An, Synthesis and structure-activity relationship of furoquinolinediones as inhibitors of Tyrosyl-DNA phosphodiesterase 2 (TDP2), Eur. J. Med. Chem. 151 (2018) 777–796.
[12] K. Moonen, I. Laureyn, C.V. Stevens, Synthetic methods for azaheterocyclic phosphonates and their biological activity, Chem. Rev. 104 (2004) 6177–6215.
[13] S. Van der Jeught, C.V. Stevens, Direct phosphonylation of aromatic azaheterocycles, Chem. Rev. 109 (2009) 2672–2702.
[14] L. Chen, X.-Y. Liu, Y.-X. Zou, Recent advances in the construction of phosphorus-substituted heterocycles, 2009–2019, Adv. Synth. Catal. 362 (2020) 1724–1818.

[15] P. Kafarski, B. Lejczak, Biological activity of aminophosphonic acids, Phosphorus Sulfur 63 (1991) 193–215.
[16] R. Engel, The use of carbon-phosphorus analogue compounds in the regulation of biological processes, in: R. Engel, M. Dekker (Eds.), Handbook of Organophosphorus Chemistry, 1992, pp. 559–600. New York.
[17] L.D. Quin, Organophosphorus compounds in medicine, in: A Guide to Organophosphorus Chemistry, John Wiley & Sons, New York, 2000, pp. 362–367.
[18] A.J. Wiemer, D.F. Wiemer, Prodrugs of phosphonate and phosphates: crossing the membrane barrier, in: Phosphorus Chem. I, Springer, 2014, pp. 115–160.
[19] D.L. Pompliano, E. Rands, M.D. Schaber, S.D. Mosser, N.J. Anthony, J.B. Gibbs, Steady-state kinetic mechanism of ras farnesyl: protein transferase, Biochemistry 31 (1992) 3800–3807.
[20] S. Bagchi, P. Rathee, V. Jayaprakash, S. Banerjee, Farnesyl transferase inhibitors as potential anticancer agents, Mini Rev. Med. Chem. 18 (2018) 1611–1623.
[21] A. Al-Kali, V. Gandhi, M. Ayoubi, M. Keating, F. Ravandi, Forodesine: review of preclinical and clinical data, Future Oncol. 6 (2010) 1211–1217.
[22] T. Yokomatsu, H. Abe, M. Sato, K. Suemune, T. Kihara, S. Soeda, H. Shimeno, S. Shibuya, Synthesis of 1,1-difluoro-5-(1H-9-purinyl)-2-pentenylphosphonic acids and the related methano analogues. Remarkable effect of the nucleobases and the cyclopropane rings on inhibitory activity toward purine nucleoside phosphorylase, Bioorg. Med. Chem. 6 (1998) 2495–2505.
[23] J. Modranka, T. Janecki, Efficient synthesis of phosphorylated ortho-fused azaheterocycles, Tetrahedron 67 (2011) 9595–9601.
[24] J. Kędzia, J. Modranka, T. Janecki, Efficient syntheses of 3-phosphorylquinolin-4-ones and 3-phosphoryl-1,8-naphthyridin-4-ones, Tetrahedron Lett. 52 (2011) 6623–6626.
[25] K. Gach, J. Modranka, J. Szymański, D. Pomorska, U. Krajewska, M. Mirowski, T. Janecki, A. Janecka, Anticancer properties of new synthetic hybrid molecules combining naphtho[2,3-b]furan-4,9-dione or benzo[f]indole-4,9-dione motif with phosphonate subunit, Eur. J. Med. Chem. 120 (2016) 51–63.
[26] I.A. Shaikh, F. Johnson, A.P. Grollman, Streptonigrin. 1. Structure-activity relationships among simple bicyclic analogues. Rate dependence of DNA degradation on quinone reduction potential, J. Med. Chem. 29 (1986) 1329–1340.
[27] K. Vermeulen, D.R. Van Bockstaele, Z.N. Berneman, The cell cycle: a review of regulation, deregulation and therapeutic targets in cancer, Cell Prolif 36 (2003) 131–149.
[28] M. Mashimo, M. Onishi, A. Uno, A. Tanimichi, A. Nobeyama, M. Mori, T. Fujii, The 89-kDa PARP1 cleavage fragment serves as a cytoplasmic PAR carrier to induce AIF-mediated apoptosis, J. Biol. Chem. 296 (2021) 100046.
[29] L.J. Mah, A. El-Osta, T.C. Karagiannis, γH2AX: a sensitive molecular marker of DNA damage and repair, Leukemia 24 (2010) 679–686.
[30] M. Podhorecka, A. Skladanowski, P. Bozko, H2AX phosphorylation: its role in DNA damage response and cancer therapy, J. Nucleic Acids 2010 (2010) 920161.
[31] F. Sivandzade, A. Bhalerao, L. Cucullo, Analysis of the mitochondrial membrane potential using the cationic JC-1 dye as a sensitive fluorescent probe, Bio-protocol 9 (2019) e3128.
[32] P. Srijiwangsa, K. Na-Bangchang, Roles of NAD (P) H-quinone oxidoreductase 1 (NQO1) on cancer progression and chemoresistance, J. Clin. Exp. Oncol. 6 (2017) 2.
[33] M. Schieber, N.S. Chandel, ROS function in redox signaling and oxidative stress, Curr. Biol. 24 (2014) R453–R462.
[34] V. Aggarwal, H.S. Tuli, A. Varol, F. Thakral, M.B. Yerer, K. Sak, G. Sethi, Role of reactive oxygen species in cancer progression: molecular mechanisms and recent advancements, Biomolecules 9 (2019) 735.
[35] B. Perillo, M. Di Donato, A. Pezone, E. Di Zazzo, P. Giovannelli, G. Galasso, A. Migliaccio, ROS in cancer therapy: the bright side of the moon, Exp. Mol. Med. 52 (2020) 192–203.
[36] K. Zhang, D. Chen, K. Ma, X. Wu, H. Hao, S. Jiang, NAD (P) H: quinone oxidoreductase 1 (NQO1) as a therapeutic and diagnostic target in cancer, J. Med. Chem. 61 (2018) 6983–7003.
[37] C.E. Pereyra, R.F. Dantas, S.B. Ferreira, L.P. Gomes, F.P. Silva Jr., The diverse mechanisms and anticancer potential of naphthoquinones, Canc. Cell Int. 19 (2019) 1–20.
[38] Y. Ling, Q.X. Yang, Y.N. Teng, S. Chen, W.J. Gao, J. Guo, K.H. Lee, Development of novel amino-quinoline-5, 8-dione derivatives as NAD (P) H: quinone oxidoreductase 1 (NQO1) inhibitors with potent antiproliferative activities, Eur. J. Med. Chem. 154 (2018) 199–209.
[39] T. Mosmann, Rapid colorimetric assay for cellular growth and survival: application to proliferation and cytotoxicity assays, J. Immunol. Methods 65 (1983) 55–63.